

Proton electromagnetic form factors and radii from lattice QCD

Miguel Salg, Dalibor Djukanovic, Georg von Hippel, Harvey B. Meyer, Konstantin Ottnad,
Hartmut Wittig

[PRD **109**, 094510], [PRL **132**, 211901]

[arXiv:2309.17232v2] (accepted for publication in PRD)

μ ASTI, June 15, 2024

- 1 Motivation
- 2 Lattice setup
- 3 Data analysis
- 4 Model average and final results
- 5 Conclusions and outlook

- Precision matters if lattice QCD is to have an impact on determination of the proton radii
- In lattice QCD as in the context of scattering experiments: electromagnetic radii extracted from the slope of the corresponding form factors at $Q^2 = 0$,

$$\langle r^2 \rangle = -\frac{6}{G(0)} \left. \frac{\partial G(Q^2)}{\partial Q^2} \right|_{Q^2=0} \quad (1)$$

- Full calculation of the proton and neutron form factors separately necessitates explicit treatment of the numerically challenging quark-disconnected contributions
- Neglected in many previous lattice studies, in particular no simultaneous control of all relevant systematics (continuum and infinite-volume extrapolation)
- Accurate determination of proton radii from muonic hydrogen spectroscopy \Rightarrow other definitions of radii, not previously computed on the lattice, become relevant

- Lamb shift

- LO proton-structure contribution: electric radius
- NLO: two-photon exchange, dominated by elastic part, depends on third Zemach moment¹,

$$\langle r_E^3 \rangle_{(2)}^p = \frac{24}{\pi} \int_0^\infty \frac{dQ^2}{(Q^2)^{5/2}} \left[(G_E^p(Q^2))^2 - 1 + \frac{1}{3} \langle r_E^2 \rangle^p Q^2 \right] \quad (2)$$

- Associated radius: Friar radius, $r_F^p = \sqrt[3]{\langle r_E^3 \rangle_{(2)}^p}$

- Hyperfine splitting (HFS)

- LO proton-structure contribution: Zemach radius²,

$$r_Z^p = -\frac{2}{\pi} \int_0^\infty \frac{dQ^2}{(Q^2)^{3/2}} \left(\frac{G_E^p(Q^2)G_M^p(Q^2)}{\mu_M^p} - 1 \right) \quad (3)$$

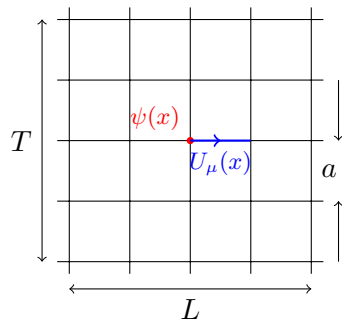
- First-principles prediction of Zemach radius could be checked by high-precision experiments

¹Friar 1979 [Ann. Phys. 122, 151]; ²Zemach 1956 [Phys. Rev. 104, 1771].

- 1 Motivation
- 2 Lattice setup**
- 3 Data analysis
- 4 Model average and final results
- 5 Conclusions and outlook

QCD on the lattice

- Coupling of QCD is large at large distances / low energies
- Low-energy regime of QCD (typical hadronic scales) is hence inaccessible to perturbative methods
- Powerful tool for the non-perturbative study: lattice QCD
- Replace space-time by a four-dimensional Euclidean lattice
- Gauge-invariant UV-regulator for the quantum field theory due to the momentum cut-off
- Path integral becomes finite-dimensional and can be computed numerically
- Allows a systematic extrapolation to the continuum and infinite-volume limit, $a \rightarrow 0$ and $V \rightarrow \infty$



Coordinated Lattice Simulations (CLS)³

- Non-perturbatively $\mathcal{O}(a)$ -improved Wilson fermions
- $N_f = 2 + 1$: 2 degenerate light quarks ($m_u = m_d$), 1 heavier strange quark ($m_s > m_{u,d}$)
- $\text{tr } M_q = 2m_l + m_s = \text{const.}$
- Tree-level improved Lüscher-Weisz gauge action
- $\mathcal{O}(a)$ -improved conserved vector current

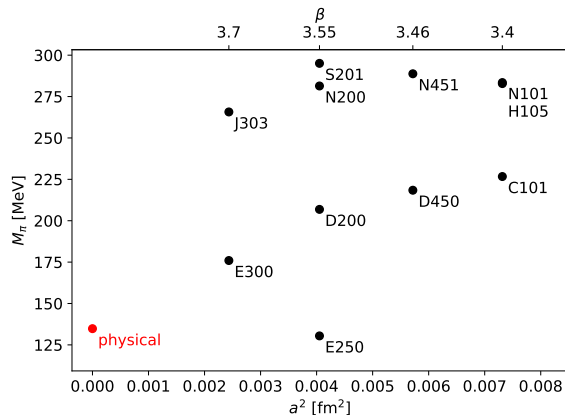
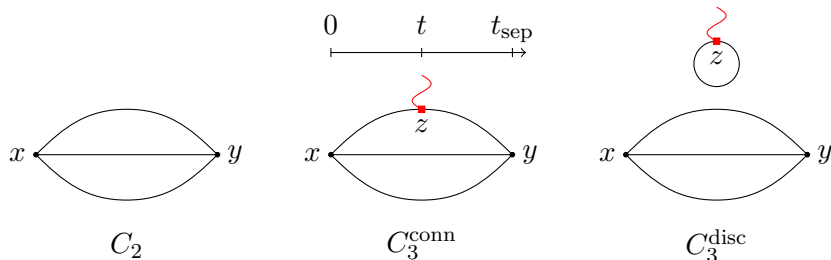


Figure: Overview of the ensembles used in this study

³Bruno et al. 2015 [[JHEP 2015 \(2\), 43](#)]; Bruno, Korzec, and Schaefer 2017 [[PRD 95, 074504](#)].

Nucleon two- and three-point correlation functions



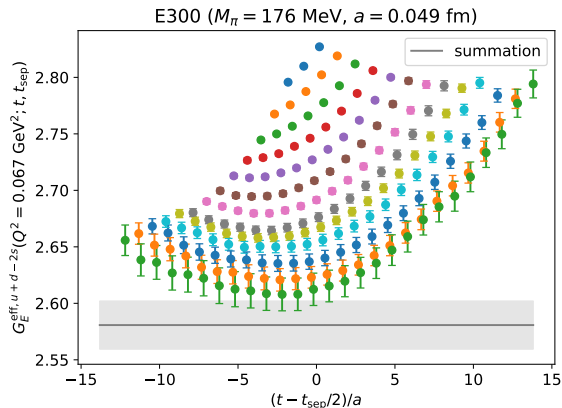
- Measure the two- and three-point correlation functions of the nucleon
- For three-point functions, Wick contractions yield connected and disconnected contribution
- Compute the quark loops via a stochastic estimation using a frequency-splitting technique⁴
- Extract the effective form factors $G_{E,M}^{\text{eff}}$ using the ratio method⁵

⁴Giusti et al. 2019 [EPJC 79, 586]; Cè et al. 2022 [JHEP 2022 (8), 220]; ⁵Korzec et al. 2009 [PoS 066, 139].

- 1 Motivation
- 2 Lattice setup
- 3 Data analysis**
- 4 Model average and final results
- 5 Conclusions and outlook

Excited-state analysis

- Cannot construct exact interpolating operator for the proton (any hadron) on the lattice
- All possible states with the same quantum numbers contribute
- Effect of heavier excited states suppressed exponentially with the distance between operators in Euclidean time
- For baryons, the relative statistical noise grows also exponentially with the source-sink separation
 $t_{\text{sep}} = y_0 - x_0$



Excited-state analysis: summation method

- Explicit treatment of the excited-state systematics required
- Summation of the effective form factors over the operator insertion time,

$$S_{E,M}(Q^2; t_{\text{sep}}) = \sum_{t=t_{\text{skip}}}^{t_{\text{sep}}-t_{\text{skip}}} G_{E,M}^{\text{eff}}(Q^2; t, t_{\text{sep}}), \quad t_{\text{skip}} = 2a \quad (4)$$

- Parametrically suppresses the effects of excited states ($\propto e^{-\Delta t_{\text{sep}}}$ instead of $\propto e^{-\Delta t}$, $e^{-\Delta(t_{\text{sep}}-t)}$ [Δ : energy gap to lowest-lying excited state]) \rightarrow “summation method”
- For $t_{\text{sep}} \rightarrow \infty$, the slope as a function of t_{sep} is given by the ground-state form factor,

$$S_{E,M}(Q^2; t_{\text{sep}}) \xrightarrow{t_{\text{sep}} \rightarrow \infty} C_{E,M}(Q^2) + \frac{1}{a}(t_{\text{sep}} + a - 2t_{\text{skip}})G_{E,M}(Q^2) \quad (5)$$

Excited-state analysis: window average

- Apply summation method with varying starting values $t_{\text{sep}}^{\text{min}}$ for the linear fit
- Perform a weighted average over $t_{\text{sep}}^{\text{min}}$, where the weights are given by a smooth window function⁶,

$$\hat{G} = \frac{\sum_i w_i G_i}{\sum_i w_i}, \quad w_i = \tanh \frac{t_i - t_w^{\text{low}}}{\Delta t_w} - \tanh \frac{t_i - t_w^{\text{up}}}{\Delta t_w}, \quad (6)$$

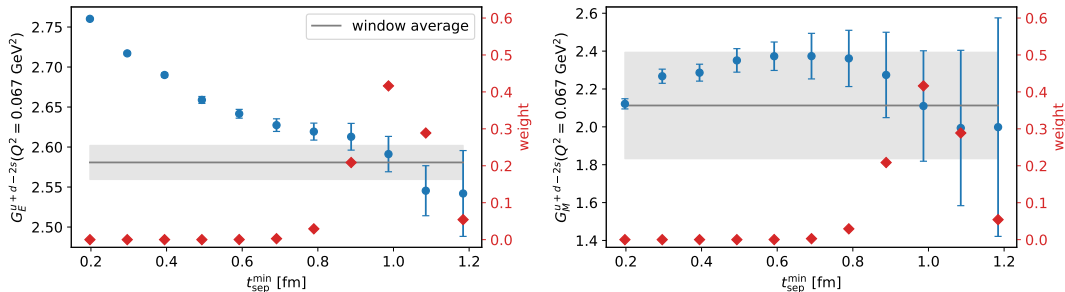
where t_i is the value of $t_{\text{sep}}^{\text{min}}$ in the i -th fit, $t_w^{\text{low}} = 0.9$ fm, $t_w^{\text{up}} = 1.1$ fm and $\Delta t_w = 0.08$ fm

⁶Djukanovic et al. 2022 [[PRD 106, 074503](#)]; Agadjanov et al. 2023 [[PRL 131, 261902](#)].

Excited-state analysis: window average

- Apply summation method with varying starting values $t_{\text{sep}}^{\text{min}}$ for the linear fit
- Perform a weighted average over $t_{\text{sep}}^{\text{min}}$, where the weights are given by a smooth window function⁶

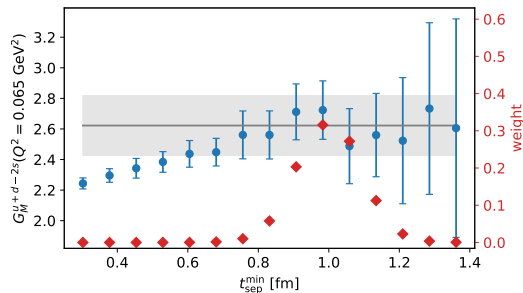
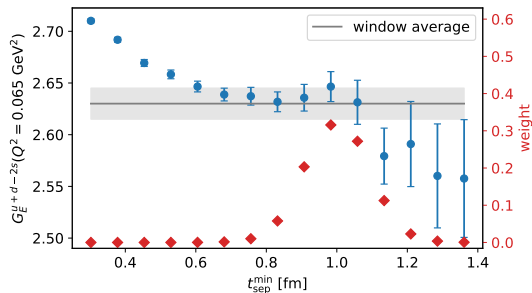
E300 ($M_\pi = 176$ MeV, $a = 0.049$ fm)



⁶Djukanovic et al. 2022 [[PRD 106, 074503](#)]; Agadjanov et al. 2023 [[PRL 131, 261902](#)].

Excited-state analysis: window average

D450 ($M_\pi = 218$ MeV, $a = 0.076$ fm)

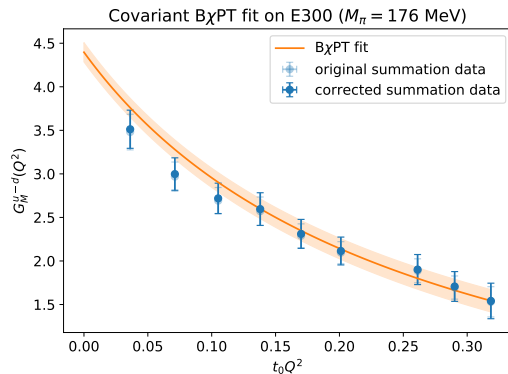
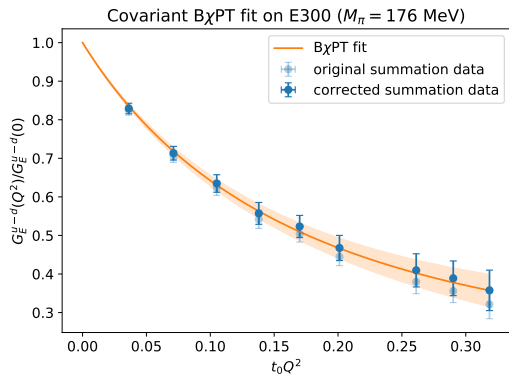


- Reliable detection of the plateau with reduced human bias (same window on all ensembles)
- Conservative error estimate

- $\langle r^2 \rangle = -\frac{6}{G(0)} \left. \frac{\partial G(Q^2)}{\partial Q^2} \right|_{Q^2=0}$, $\mu_M = G_M(0) \Rightarrow$ parametrize Q^2 -dependence of FFs
- Combine this with the chiral, continuum, and infinite-volume extrapolation
- Use expressions from covariant chiral perturbation theory⁷ to perform a simultaneous fit to the pion-mass, Q^2 -, lattice-spacing, and finite-volume dependence of the form factors
- Include contributions from the ρ (ω and ϕ) mesons in the isovector (isoscalar) channel
- Reconstruct proton and neutron observables from separate fits to the isovector and isoscalar form factors
- Perform fits with various cuts in M_π and Q^2 , as well as with different models for the lattice-spacing and finite-volume dependence, in order to estimate systematic uncertainties
- Large number of degrees of freedom \Rightarrow improved stability against lowering the Q^2 -cut

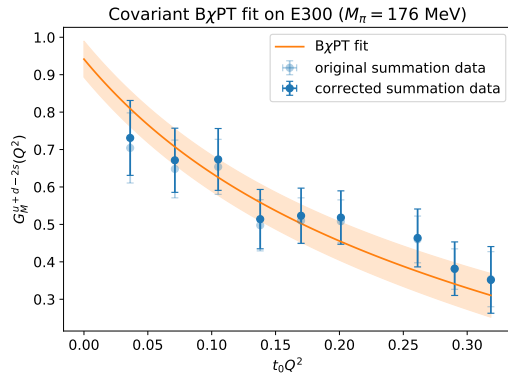
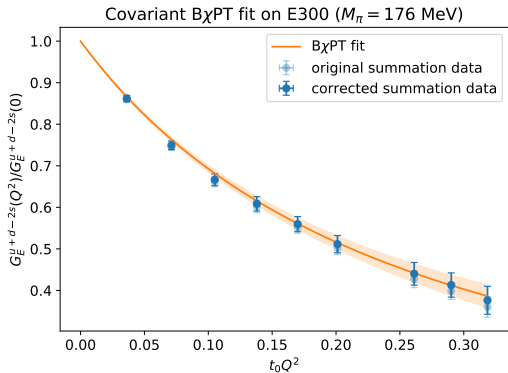
⁷Bauer, Bernauer, and Scherer 2012 [[PRC 86, 065206](#)].

Q^2 -dependence of the isovector form factors on E300



- Direct $B\chi$ PT fit describes data very well
- Reduced error due to the inclusion of several ensembles in one fit

Q^2 -dependence of the isoscalar form factors on E300



Zemach and Friar radii from the lattice

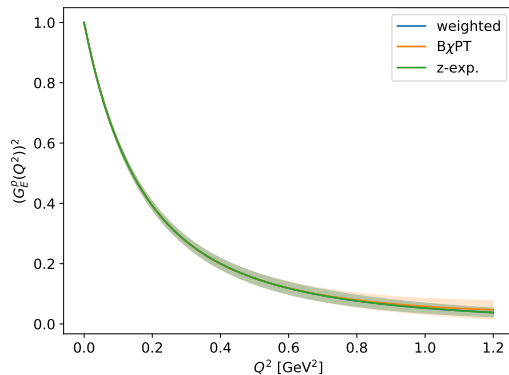
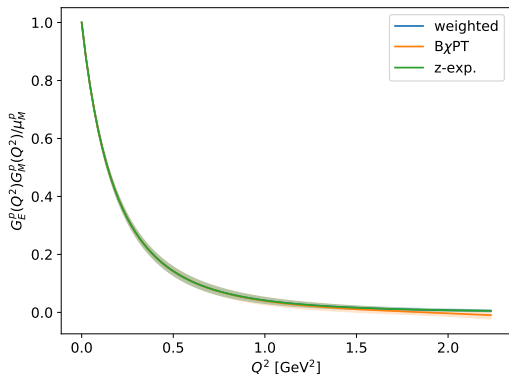
- $B\chi$ PT including vector mesons only trustworthy for $Q^2 \lesssim 0.6 \text{ GeV}^2$
- Tail of the integrands suppressed: contribution of the form factors above 0.6 GeV^2 to r_Z^p less than 0.9%, to $\langle r_E^3 \rangle_{(2)}^p$ less than 0.3%
- Extrapolate $B\chi$ PT fit results using a z -expansion⁸ *ansatz*
- Incorporate the large- Q^2 constraints on the form factors⁹
- For integration, smoothly replace $B\chi$ PT parametrization of the form factors by z -expansion-based extrapolation ($\Delta Q_w^2 = 0.1 \text{ GeV}^2$),

$$F(Q^2) = \frac{1}{2} \left[1 - \tanh \left(\frac{Q^2 - Q_{\text{cut}}^2}{\Delta Q_w^2} \right) \right] F^x(Q^2) + \frac{1}{2} \left[1 + \tanh \left(\frac{Q^2 - Q_{\text{cut}}^2}{\Delta Q_w^2} \right) \right] F^z(Q^2), \quad (7)$$

where $F(Q^2) \equiv G_E(Q^2)G_M(Q^2)/\mu_M$ for r_Z and $F(Q^2) \equiv G_E^2(Q^2)$ for $\langle r_E^3 \rangle_{(2)}$, resp.

⁸Hill and Paz 2010 [PRD 82, 113005]; ⁹Lepage and Brodsky 1980 [PRD 22, 2157]; Lee, Arrington, and Hill 2015 [PRD 92, 013013].

Integrands for the Zemach radius and third Zemach moment of the proton



- B χ PT clearly not reliable for large Q^2
- z -expansion agrees well with B χ PT parametrization in region where it is fitted

- 1 Motivation
- 2 Lattice setup
- 3 Data analysis
- 4 Model average and final results**
- 5 Conclusions and outlook

Model average

- Perform a weighted average over the results of all fit variations, using weights derived from the Akaike Information Criterion¹⁰,

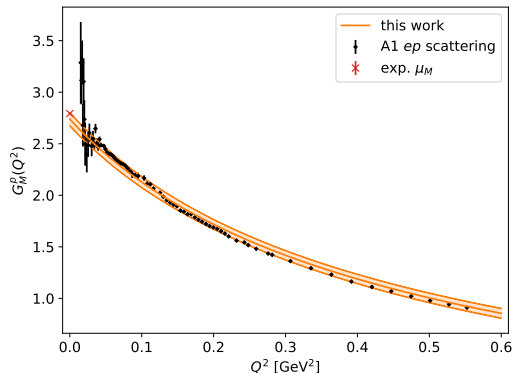
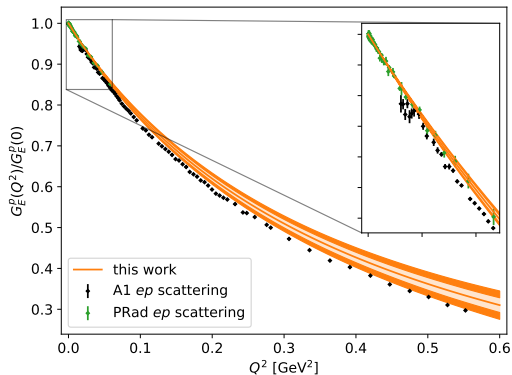
$$w_i = \exp\left(-\frac{1}{2}\text{BAIC}_i\right) / \sum_j \exp\left(-\frac{1}{2}\text{BAIC}_j\right), \quad \text{BAIC}_i = \chi_{\text{noaug,min},i}^2 + 2n_{f,i} + 2n_{c,i}, \quad (8)$$

where n_f is the number of fit parameters and n_c the number of cut data points

- Strongly prefers fits with low n_c , *i.e.*, the least stringent cut in $Q^2 \Rightarrow$ apply a flat weight over the different Q^2 -cuts to ensure strong influence of our low-momentum data
- Determine the final cumulative distribution function (CDF) from the weighted sum of the bootstrap distributions¹¹
- Quote median of this CDF together with the central 68% percentiles

¹⁰Akaike 1974 [[IEEE Trans. Autom. Contr.](#) **19**, 716]; Neil and Sitison 2022 [[arXiv:2208.14983](#)]; ¹¹Borsányi et al. 2021 [[Nature](#) **593**, 51].

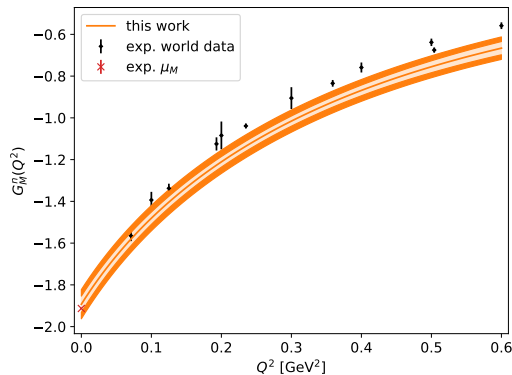
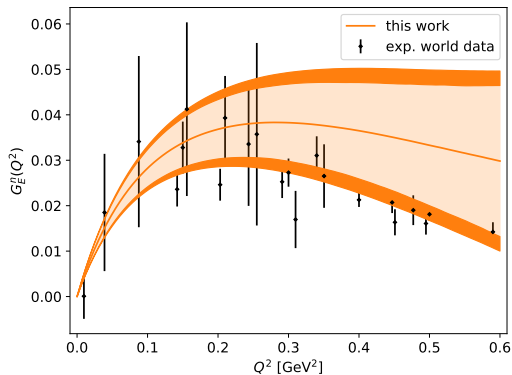
Model-averaged proton form factors at the physical point



- Slope of the electric form factor closer to that of PRad¹² than to that of A1¹³
- Good agreement with A1 for the magnetic form factor

¹²Xiong et al. 2019 [[Nature 575, 147](#)]; ¹³Bernauer et al. 2014 [[PRC 90, 015206](#)].

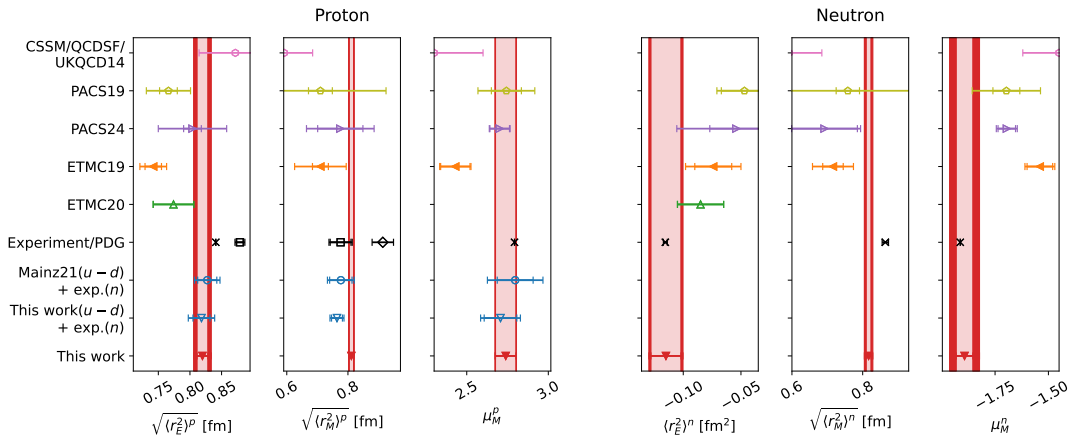
Model-averaged neutron form factors at the physical point



(Mostly) compatible with the collected experimental world data¹⁴ within our errors

¹⁴Ye et al. 2018 [PLB 777, 8].

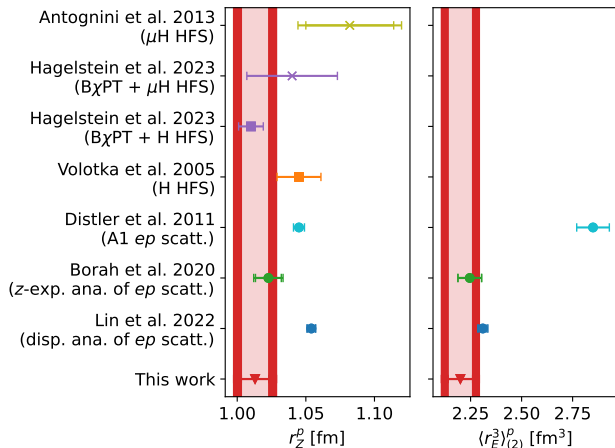
Electromagnetic radii and magnetic moments



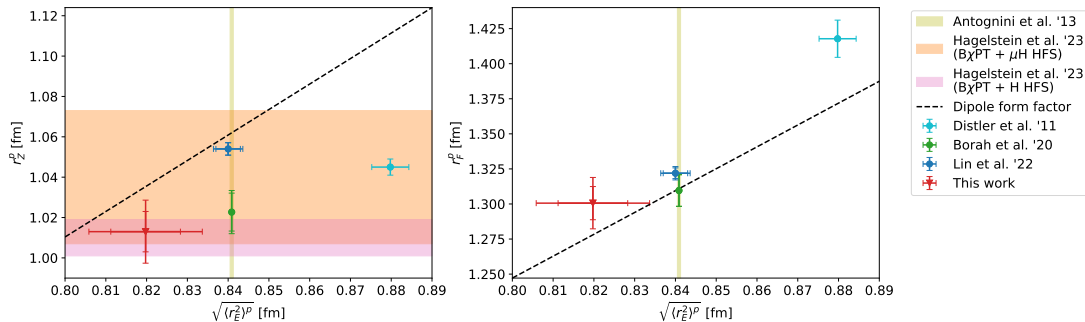
Magnetic moments reproduced, low value for $\sqrt{\langle r_E^2 \rangle^p}$ clearly favored, $\sqrt{\langle r_M^2 \rangle^p}$ agrees with A1

Zemach radii and third Zemach moments

- r_Z^p : low value favored, but agrees within 2σ with most other determinations (except for dispersive analysis)
- $\langle r_E^3 \rangle_{(2)}^p$: low value favored, good agreement with dispersive analysis, clear tension with A1
- Our estimates are $\sim 80\%$ and $\sim 95\%$, respectively, correlated with electromagnetic radii
- Low results for r_Z^p and $\langle r_E^3 \rangle_{(2)}^p$ expected, no independent puzzle
- Neutron results agree with z -expansion analysis of world en -scattering data, larger error



Correlations between different proton radii



- Large correlation of Zemach and Friar radii with electromagnetic radii also in experiment
- Lattice results seem to confirm trend observed in data-driven evaluations

- 1 Motivation
- 2 Lattice setup
- 3 Data analysis
- 4 Model average and final results
- 5 Conclusions and outlook**

- Determination of the electromagnetic form factors of the proton and neutron from lattice QCD including connected and disconnected contributions, as well as a full error budget
- Magnetic moments of the proton and neutron agree well with the experimental values
- Small electric *and* magnetic radii of the proton favored
- Accordingly also small values for Zemach and Friar radii of the proton favored (large correlation with electromagnetic radii)
- Good agreement with dispersive approaches for electric properties of the proton (electric and Friar radii), tension regarding its magnetic properties (magnetic and Zemach radii)
- Competitive errors, in particular for the magnetic radii
- Further investigations required, in particular for the proton's magnetic and Zemach radii

Backup slides

From correlation functions to form factors

- Average over the forward- and backward-propagating nucleon and over x-, y-, and z-polarization for the disconnected part
- Calculate the ratios

$$R_{V_\mu}(\mathbf{q}; t_{\text{sep}}, t) = \frac{C_{3,V_\mu}(\mathbf{q}; t_{\text{sep}}, t)}{C_2(\mathbf{0}; t_{\text{sep}})} \sqrt{\frac{\bar{C}_2(\mathbf{q}; t_{\text{sep}} - t) C_2(\mathbf{0}; t) C_2(\mathbf{0}; t_{\text{sep}})}{C_2(\mathbf{0}; t_{\text{sep}} - t) \bar{C}_2(\mathbf{q}; t) \bar{C}_2(\mathbf{q}; t_{\text{sep}})}}, \quad (9)$$

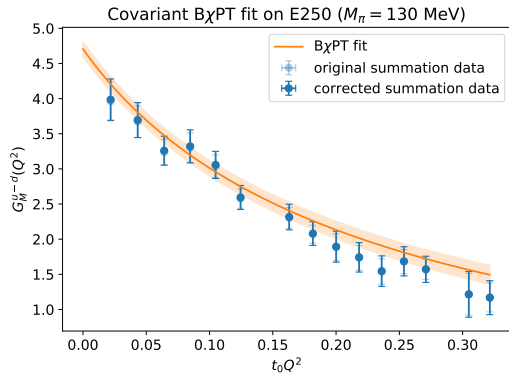
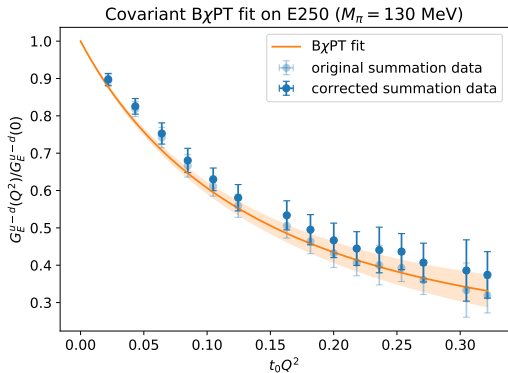
where $t_{\text{sep}} = y_0 - x_0$, $t = z_0 - x_0$, and $\bar{C}_2(\mathbf{q}; t_{\text{sep}}) = \sum_{\tilde{\mathbf{q}} \in \mathbf{q}} C_2(\tilde{\mathbf{q}}; t_{\text{sep}}) / \sum_{\tilde{\mathbf{q}} \in \mathbf{q}} 1$

- At zero sink momentum, the effective form factors can be computed from the ratios as

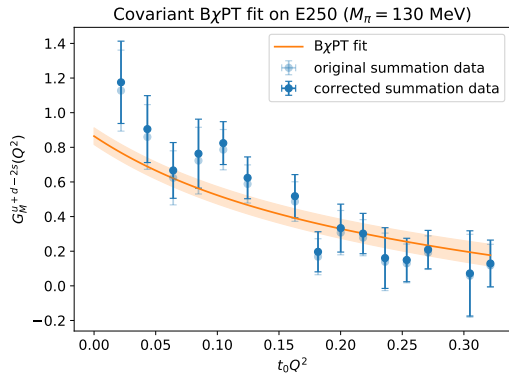
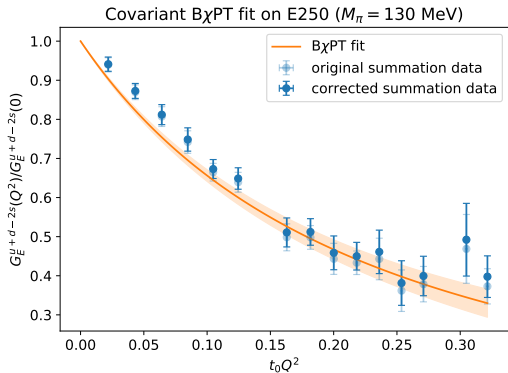
$$G_E^{\text{eff}}(Q^2; t_{\text{sep}}, t) = \sqrt{\frac{2E_{\mathbf{q}}}{m + E_{\mathbf{q}}}} R_{V_0}(\mathbf{q}; t_{\text{sep}}, t), \quad (10)$$

$$G_M^{\text{eff}}(Q^2; t_{\text{sep}}, t) = \sqrt{2E_{\mathbf{q}}(m + E_{\mathbf{q}})} \frac{\sum_{j,k} \epsilon_{ijk} q_k \text{Re} R_{V_j}^{\Gamma_i}(\mathbf{q}; t_{\text{sep}}, t)}{\sum_{j \neq i} q_j^2} \quad (11)$$

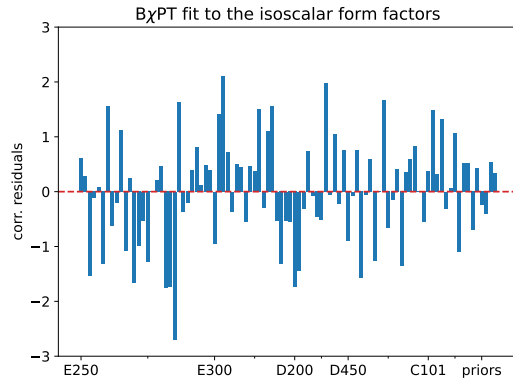
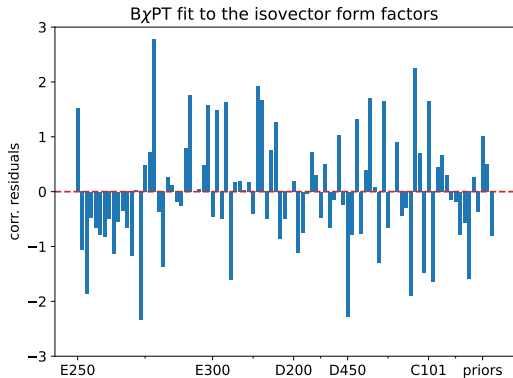
Q^2 -dependence of the isovector form factors on E250



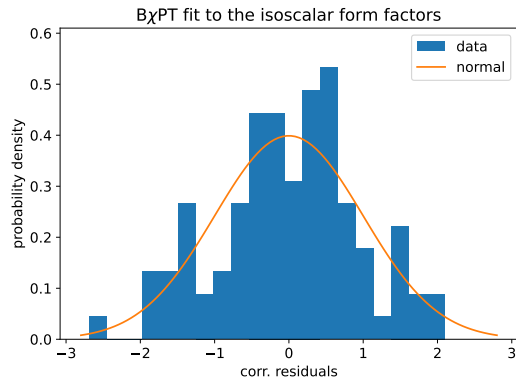
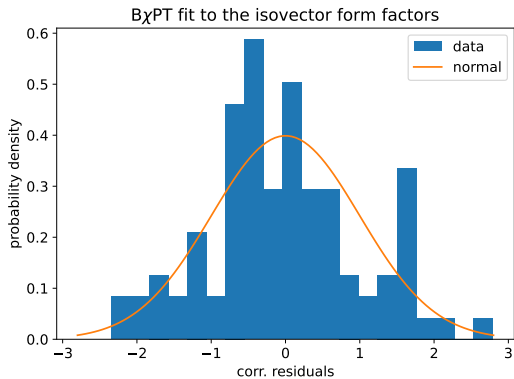
Q^2 -dependence of the isoscalar form factors on E250



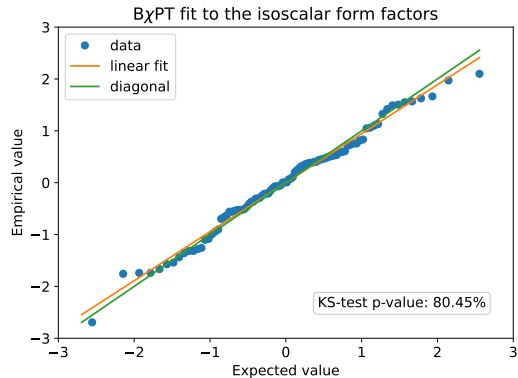
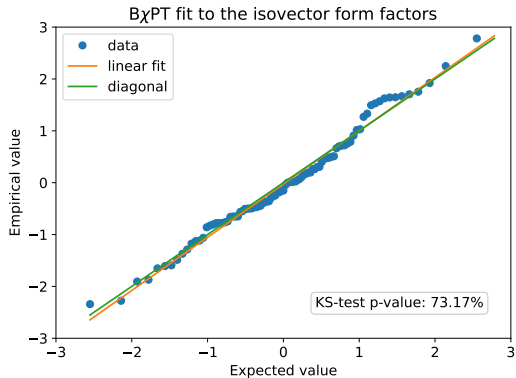
Residuals of the $B\chi$ PT fits



Histograms



Q-Q plots

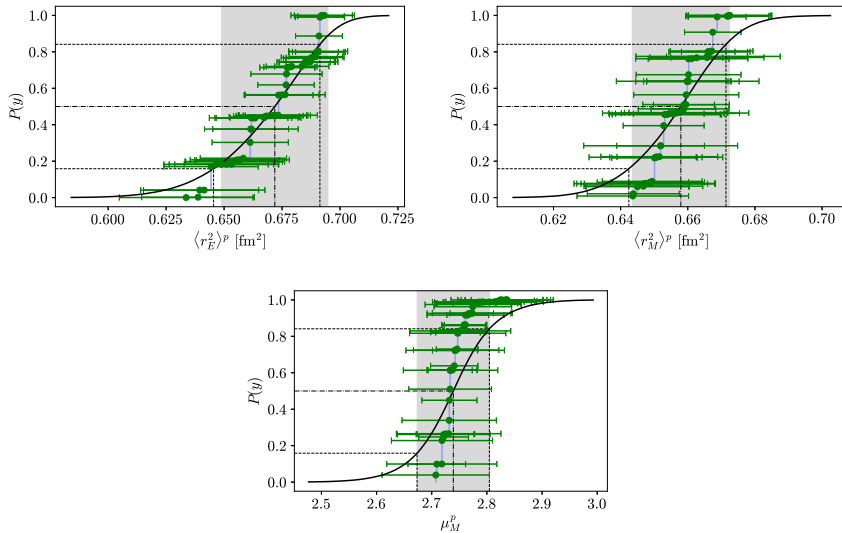


- Scale the statistical variances of the individual fit results by a factor of $\lambda = 2$
- Repeat the model averaging procedure
- Assumptions:
 - Above rescaling only affects the statistical error of the averaged result
 - Statistical and systematic errors add in quadrature
- Contributions of the statistical and systematic errors to the total error,

$$\sigma_{\text{stat}}^2 = \frac{\sigma_{\text{scaled}}^2 - \sigma_{\text{orig}}^2}{\lambda - 1}, \quad \sigma_{\text{syst}}^2 = \frac{\lambda \sigma_{\text{orig}}^2 - \sigma_{\text{scaled}}^2}{\lambda - 1} \quad (12)$$

- Consistency check: results are almost independent of λ (if it is chosen not too small)

CDFs of the electromagnetic radii and magnetic moment of the proton



Observable	Isovector	Isoscalar	Proton	Neutron
$\langle r_E^2 \rangle$ [fm ²]	0.785(22)(26)	0.554(18)(13)	0.672(14)(18)	-0.115(13)(7)
$\langle r_M^2 \rangle$ [fm ²]	0.663(11)(8)	0.657(30)(31)	0.658(12)(8)	0.667(11)(16)
μ_M	4.62(10)(7)	2.47(11)(10)	2.739(63)(18)	-1.893(39)(58)
r_Z [fm]	-	-	1.013(10)(12)	-0.0411(56)(40)
$\langle r_E^3 \rangle_{(2)}$ [fm ³]	-	-	2.200(60)(71)	0.0078(20)(12)

- z -expansion: model-independent description of the Q^2 -dependence of the form factors
- Map domain of analyticity of the form factors onto the unit circle,

$$z(Q^2) = \frac{\sqrt{\tau_{\text{cut}} + Q^2} - \sqrt{\tau_{\text{cut}} - \tau_0}}{\sqrt{\tau_{\text{cut}} + Q^2} + \sqrt{\tau_{\text{cut}} - \tau_0}}, \quad (13)$$

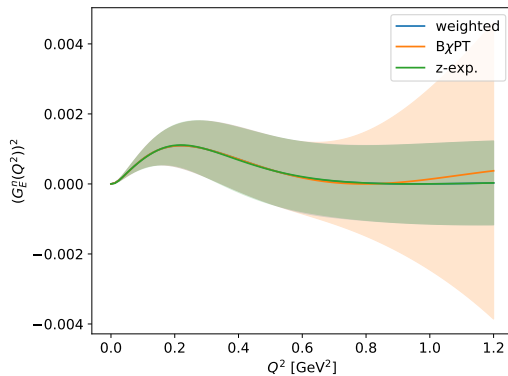
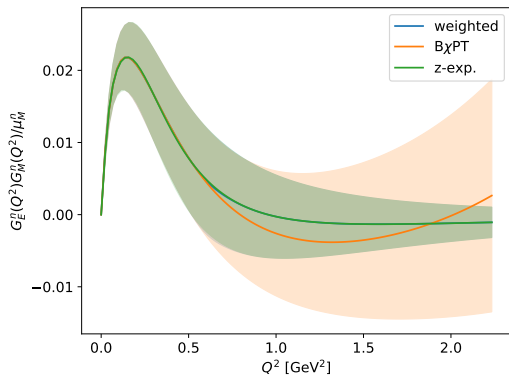
where $\tau_{\text{cut}} = 4M_{\pi, \text{phys}}^2$, and we employ $\tau_0 = 0$

- Expand the form factors as

$$G_E^{p,n}(Q^2) = \sum_{k=0}^m a_k^{p,n} z(Q^2)^k, \quad G_M^{p,n}(Q^2) = \sum_{k=0}^m b_k^{p,n} z(Q^2)^k \quad (14)$$

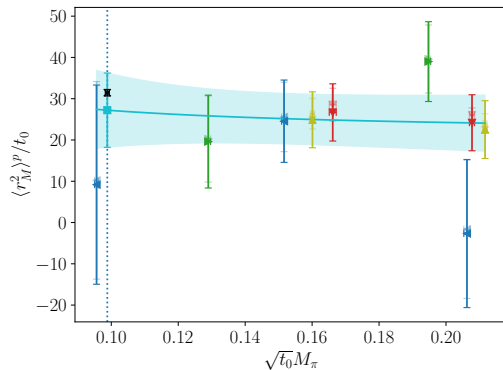
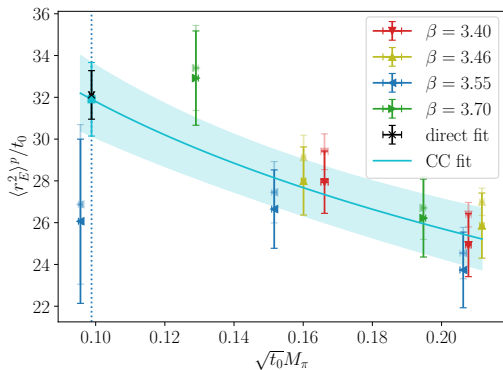
- We fix $G_E^p(0) = a_0^p = 1$ and $G_E^n(0) = a_0^n = 0$, respectively, use $m = 9$, and incorporate the 4 sum rules for each form factor

Integrands for the Zemach radius and third Zemach moment of the neutron



z -expansion agrees also here well with B χ PT parametrization in region where it is fitted

Crosscheck of direct fits with z -expansion: proton electromagnetic radii



Radii in good agreement with direct fits, albeit with significantly larger errors